Society of Medical Education & Research

2024, Volume 4, Issue 2, Page No: 167-185
ISSN: 3108-4834

Archive of International Journal of Cancer and Allied Science

Mutant KRAS Drives Loss of S100PBP Expression, Enhancing Pancreatic Cancer Progression and Poor Prognosis

Pedro Henrique Monteiro[1]*, Lucas André Ferreira[1]

[1]Oncology Research Unit, Federal University of Minas Gerais, Belo Horizonte, Brazil.

***E-mail** ✉ p.monteiro.ufmg@yahoo.com

Abstract

Previous research indicated a gradual reduction in the levels of S100P-binding protein (S100PBP) during the progression of pancreatic ductal adenocarcinoma (PDAC). In this study, we show that the loss of S100PBP contributes to the transformation of pancreatic cells into oncogenic forms. Both computational and laboratory analyses revealed that deregulation of S100PBP expression impacts several genes involved in the regulation of the cytoskeleton, cell movement, and survival. Overexpression of S100P suppressed S100PBP levels, and co-immunoprecipitation experiments suggested that S100P interacts with the S100PBP-p53-ubiquitin complex, potentially leading to its degradation. Activation of KrasG12D with doxycycline resulted in lower S100PBP levels, which were restored by treating with the HDAC inhibitor MS-275 in both human and murine PDAC cell lines. This suggests KrasG12D regulates S100PBP at an epigenetic level. Additionally, TCGA PanCancer Atlas PDAC datasets showed that low levels of S100PBP and high levels of S100P correlate with poor prognosis in patients, positioning S100PBP as a potential tumor suppressor with clinical relevance.

Keywords: Pancreatic cancer, Cytoskeleton, Tumor, Clinical relevance

Introduction

In our previous work, we discovered a novel binding partner for the S100P protein, S100PBP, which is widely expressed and lacks homology to any known proteins [1]. We showed that silencing S100PBP led to an increase in CTSZ levels, while overexpressing it resulted in decreased CTSZ levels, with S100PBP facilitating cell adhesion through CTSZ and αvβ5 integrin interaction [2]. Limited research has been conducted on S100PBP so far. Our bioinformatic analysis of pancreatic cancer transcriptomics [3] highlighted its involvement in regulating miRNA pathways, cytoskeletal organization, and suppression of cell migration and invasion. Additionally, S100PBP has been identified as a target for miR-944, a miRNA linked to increased cell proliferation and invasion in cervical cancer [4]. Moreover, S100PBP is part of a three-gene signature predictive of relapse-free survival in colorectal cancer patients after liver metastasis surgery [5]. Despite these findings, the full biological functions of S100PBP remain unclear.

In pancreatic tissue, S100PBP is expressed in both the exocrine and endocrine regions, primarily in the nucleus [1, 2]. However, during pancreatic intraepithelial neoplasia (PanIN) progression, a precursor to PDAC, S100PBP expression is reduced or mislocalized to the cytoplasm. This loss of S100PBP expression is inversely correlated with increasing levels of S100P, an oncogenic protein [1, 2]. Given that S100P overexpression is associated with increased motility and invasiveness [6], we hypothesized that S100PBP may play a role in regulating these processes.

Access this article online https://smerpub.com/

Received: 14 September 2024; **Accepted:** 08 December 2024

How to cite this article: Monteiro PH, Ferreira ML. Mutant KRAS Drives Loss of S100PBP Expression, Enhancing Pancreatic Cancer Progression and Poor Prognosis. Arch Int J Cancer Allied Sci. 2024;4(2):167-85. https://doi.org/10.51847/FrbLuzb4Yz

This study investigates the role of S100PBP in controlling cell morphology, motility, invasion, and survival, potentially positioning it as a novel tumor suppressor.

Materials and Methods

Cell culture

Human pancreatic ductal adenocarcinoma (PDAC) cell lines (CFPac1, Panc1, MIA PaCa2, PaTu-8988s/t), chronic myeloid leukemia (CML) cell lines (HAP1 parental and HAP1 CRISPR-Cas9 S100PBP knockout cells from Horizon Discovery, UK), and doxycycline-inducible KrasG12D PDAC mouse cell lines [7] were cultured in their appropriate media with 10% fetal bovine serum (FBS) and Penicillin/Streptomycin in a humidified incubator. The mouse PDAC cell lines received doxycycline (100 µg/ml) for 48 hours prior to analysis of proteins and RNA. Cell line identity was confirmed by short tandem repeat (STR) profiling. Phase contrast images were taken at 10x magnification using an Olympus light microscope (Germany).

Western blotting

To examine protein expression differences among the cell lines based on S100PBP expression levels or after manipulation, Western blotting was performed according to the previously outlined method [8]. In brief, 50 µg of cell lysate was separated by SDS-PAGE on 7.5%–15% polyacrylamide gels, and transferred to nitrocellulose membranes (0.2 µm pore size, GE Healthcare, UK). With chemiluminescence detection (Millipore, UK). Protein levels were quantified using ImageJ software, with fold changes relative to control groups indicated above the bands in the blots.

qPCR

Quantitative PCR (qPCR) was carried out to assess gene expression levels, as described previously [8]. RNA was extracted using Tripure reagent (Roche, USA) and quantified. For cDNA synthesis, 2 µg of RNA was reverse transcribed using a single strand synthesis kit (Roche, USA). The qPCR reactions were performed using SYBR Green (Applied Biosciences, UK), on an ABI 7500 real-time PCR machine (Applied Biosciences, UK).

Immunofluorescence staining

F-actin localization was analyzed by staining cells with Rhodamine-phalloidin (Life Technologies, UK), following the procedure outlined previously [9]. F-actin intensity per cell was quantified using Adobe Photoshop 2021 software, with data presented as average intensity per cell beneath each image. Other proteins were detected using an LSM710 confocal microscope (Zeiss, Germany) as described before [8, 10].

Migration and invasion assays

Cell migration was assessed by plating 0.5 × 10^6 cells on collagen-I-coated 6-well plates, followed by mitomycin C (2 µg/ml) treatment for 2 hours, and scratching the cells to create wound gaps, as previously described [10]. Migration and wound closure were tracked by capturing time-lapse images with an Axio-Vision microscope (UK) at 10x magnification. For invasion assays, 5 × 10^4 cells in serum-free DMEM were seeded onto Matrigel-coated transwell inserts (0.8 µm pore size) in 24-well plates and incubated for 48 hours. Cells that passed through the pores were fixed with methanol and stained with Giemsa blue. Five representative images per insert were captured at 20x magnification using an Olympus light microscope.

Gene silencing by siRNA

S100PBP expression was silenced in Panc1 and MIA PaCa2 cells using 50 nM siRNA. In brief, 0.5 × 10^6 cells were seeded and transfected with either scrambled (non-target) or specific siRNAs against S100PBP (Mol1: AUGGUGGUUCACACAAGUCAA, Mol2: CUGUGUGAGUAAUGCAUUCUA; Qiagen, UK) using RNAiMax reagent (Life Technologies, UK). After 16 hours, the medium was changed, and cells were harvested after 72 hours for protein and RNA analysis. A subset of cells was cultured on coverslips for further immunofluorescence studies.

Stable gene overexpression

To establish stable overexpression of S100PBP in low-expressing cells (CFPac1 and PaTu-8988t), we used the pCMV-Tag2B expression vector carrying the full-length S100PBP gene and an empty vector (EV) [1, 2]. Similarly, Panc1 cells stably expressing S100P were generated using the pcDNA3.1 vector carrying full-length S100P. Briefly, 0.2 × 10^6 cells per well were seeded in 6-well plates and transfected with the plasmid-FuGene6 (Promega, UK) complexes for 48 hours.

Transfected cells were selected using 1.1 mg/ml geneticin (G418 sulfate; InvivoGen, UK) for 3 weeks. Gene expression was confirmed by both mRNA and protein analysis.

Co-immunoprecipitation

To explore protein interactions, we performed co-immunoprecipitation. In brief, 4 µg of rabbit polyclonal antibodies (anti-S100PBP and IgG) were linked to protein G-coated Dynabeads (Life Technologies, UK) according to the manufacturer's protocol. The antibody-Dynabead complexes were incubated with whole-cell lysates (15 × 10^6 cells in NP-40 buffer) under constant rotation at 4°C for 24 hours. After incubation, magnetic separation was employed to isolate the antibody-protein complex. The proteins were then eluted in a non-denaturing manner, with Laemmli buffer (Sigma-Aldrich, UK) added to both the eluted sample and the input (2% of total lysate). Western blotting was used to detect the proteins.

In silico analysis

RNA was isolated from MIA PaCa-2 and FA6 cells following alterations in S100PBP expression as previously described [2], and gene expression profiling was conducted. The data have been deposited in the Gene Expression Omnibus (GEO) with accession number GSE35199 (https://www.ncbi.nlm.nih.gov/geo).

The data were analyzed using Ingenuity Pathway Analysis (IPA, Qiagen, UK) to identify connected signaling pathways. Additionally, the TCGA PanCancer Atlas dataset for PDAC (n = 177) was utilized for further analysis using the cBioPortal for Cancer Genomics (https://www.cbioportal.org/) and Protein Atlas websites (https://www.proteinatlas.org/).

Flow cytometry

Cell apoptosis was assessed using the FITC Annexin V Apoptotic Detection Kit (BD Biosciences, USA). Cells (10^5 per well) were seeded in collagen-I-coated 6-well plates and treated with gemcitabine (0.01 µM) for 72 hours. After the treatment, cells were centrifuged (500 × g for 5 minutes) and resuspended in binding buffer with FITC-labeled annexin V and propidium iodide (PI). Apoptotic cells were quantified using the LSR Fortessa-3 flow cytometer and analyzed with FACS DIVA software (BD Biosciences, USA).

Statistical analysis

All experiments were conducted in triplicate unless otherwise noted. Results are expressed as mean ± SD. Statistical significance was assessed using Student's t-test or one-way ANOVA followed by Dunnett's post-hoc test when comparing more than two groups. GraphPad Prism v8 software was used for all analyses, with a p-value of < 0.05 considered significant.

Results and Discussion

Role of S100PBP in Cell Morphology, Motility, and Invasion

Bioinformatics analysis of transcriptomic data from PDAC cell lines MIA PaCa-2 and FA6, with altered S100PBP expression [2], revealed the involvement of several signaling pathways critical for regulating cell shape, movement, and survival, such as RhoB, p53, and AKT pathways **(Figures 1 and 1b).** These results were validated in CML and PDAC cell lines: high expression of S100PBP in Panc1, MIA PaCa-2, and HAP1 parental cells corresponded with elevated RhoB, p-myosin phosphatase1 (MYPT1)-S696, and p-cofilin-S3 levels, indicating active RhoB/Rho-kinase (ROCK) signaling **(Figure 1c)**. Conversely, cells with low S100PBP expression, such as CFPac1, PaTu-8988s/t, and HAP1-S100PBP knockout cells, exhibited lower levels of these proteins **(Figure 1c)**, suggesting that S100PBP modulates RhoB/ROCK signaling. Cellular F-actin localization further supported this, with cells expressing high S100PBP showing strong cortical staining and well-formed stress fibers, while cells with low S100PBP displayed weak cortical F-actin staining and fewer stress fibers **(Figure 1d)**. The morphological changes were consistent with these findings: cells with high S100PBP had a cobblestone-like appearance, while cells with low S100PBP were more spindle-shaped with poorly defined borders.

S100PBP silencing in Mia PaCa-2 cells	Up-regulated	**AKT2**, ANXA1, CTNNB1, CTTN, ECT2, MAPK8, PRKAA1, SEPT9, PIK3C2A, JAK2, NF1, CTSZ, TCF7L2, APP, KIFC1, RTN4
	Down-regulated	CALR, CBX5,ERBB2, GSN, MYH10, **RHOB**, SFRP1, SKP2, PPARA, PTPN14, TP63, RAB35, CRKL, ARHGDIA, **S100PBP**
S100PBP over-expression in FA6 cells	Up-regulated	CAV1, CST6, CXCR4, DLC1, F2R FST, GBP1, HIPK2, GALS1, MCAM, MET, MMP1, **RHOB**, SKP2, S100A4, HBEGF, ADM, PRSS1/PRSS3, SNAI2, **TP53**, ICAM1, CDKN2A, JAG2, P2RY2 IL7, PKP3, STC1, **S100PBP**
	Down-regulated	CBX5, DIAPH2, DOCK1, ELF3, ID2, INHBB, LCN2, PLAC1, PTP4A3, SPP1, TFF1, TFF2, S100A9, **S100P**, DICER1, ITGB2, CTSZ, C3, TCF7L2, PTHLH, SERPINA5, CXCL6

a)

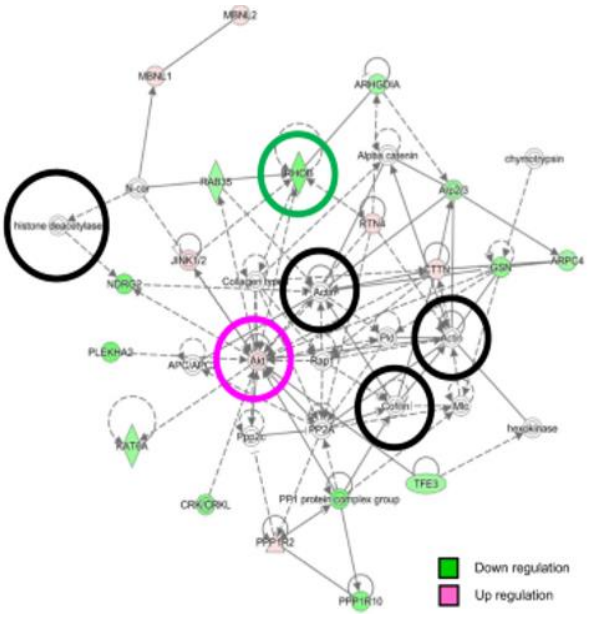

b)

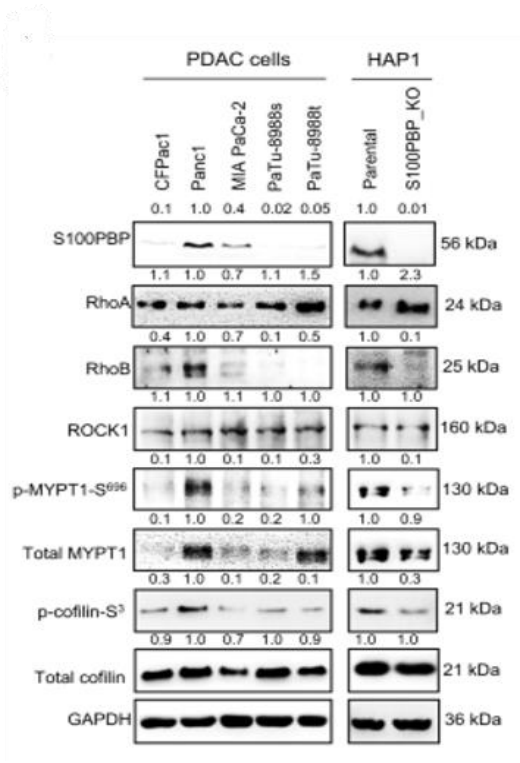

c)

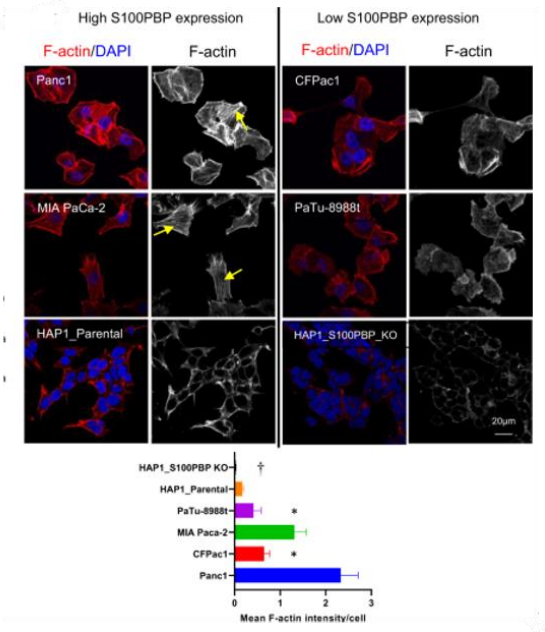

d)

Figure 1. Network analysis highlights S100PBP's role in regulating cell movement

Ingenuity Pathway Analysis (IPA) was performed on gene expression data from MIA PaCa-2 and FA6 pancreatic cancer cell lines following S100PBP expression disruption: a) Genes associated with cell

movement were filtered out, and b) Relevant networks were constructed. c) Western blotting results comparing the expression of S100PBP, RhoA, RhoB, ROCK1, p-MYPT1-S696, total MYPT1, p-cofilin-S3, and cofilin in various PDAC and HAP1 cell lines (parental vs. S100PBP knockout (KO)) showed significant differences. GAPDH served as a loading control. The fold changes in protein expression relative to controls (Panc1 and HAP1-parental) are indicated above the blots following densitometric analysis. d) Localization of F-actin and the mean signal intensity per cell were analyzed in PDAC and HAP1 cell lines. Nuclei were stained with DAPI, with arrows indicating stress fiber formation. Scale bar: 20 µm. N = 3, mean ± SD. Statistical comparisons were made between HAP1 S100PBP KO cells vs. HAP1 parental, †$p < 0.05$; low S100PBP-expressing PDAC lines vs. Panc1, *$p < 0.05$.

To further investigate how S100PBP influences cytoskeletal stability, we used two independent siRNA sequences (siRNA mol1 and mol2) to silence S100PBP in Panc1 and MIA PaCa-2 cells that naturally express S100PBP. Silencing resulted in a decrease in RhoB activity, evidenced by lower levels of RhoB, p-MYPT1-S696, and p-cofilin-S3 in the S100PBP silenced groups compared to controls treated with scrambled siRNA **(Figure 2a).** Reduced mRNA levels of RhoB in both HAP1-S100PBP knockout cells and Panc1 cells after transient S100PBP silencing suggested that S100PBP regulates RhoB transcription. These findings were further supported by F-actin localization analysis, where control Panc1 and MIA PaCa-2 cells showed intense cortical F-actin staining and well-formed stress fibers, while S100PBP-silenced cells exhibited weaker F-actin staining and lost stress fibers **(Figure 2b).** Similar F-actin patterns were observed in HAP1 cells with S100PBP knockout **(Figure 1d).**

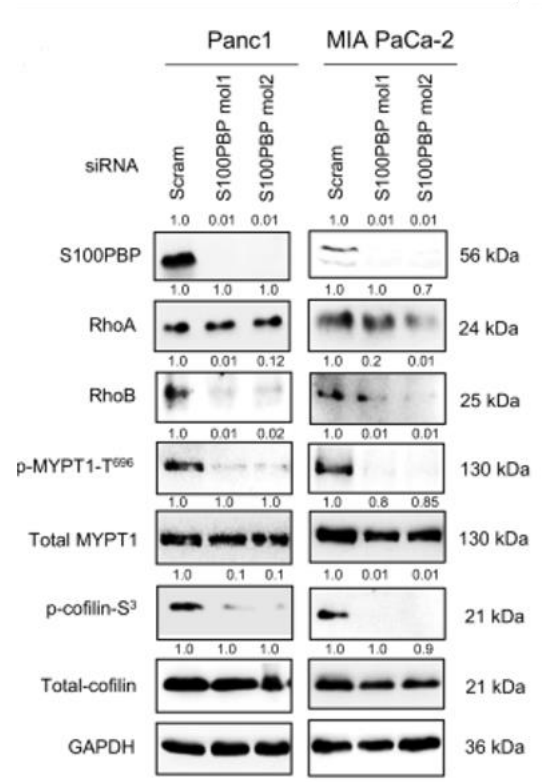

a)

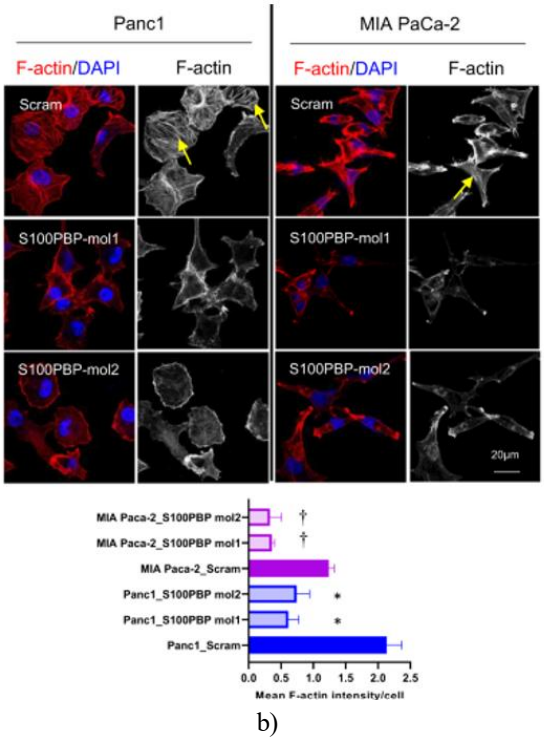

b)

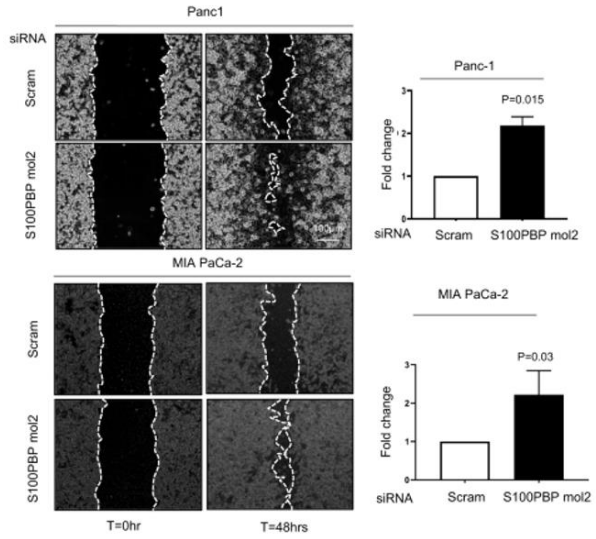

c)

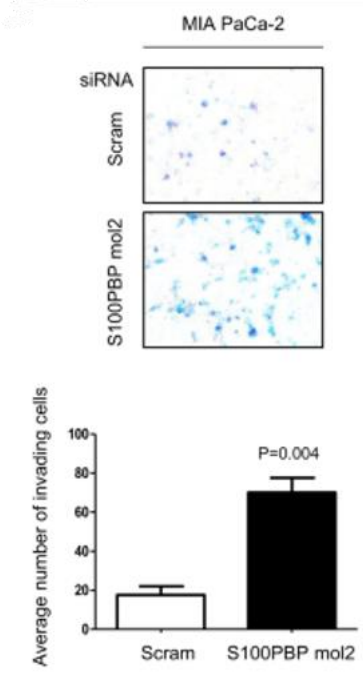

d)

Figure 2: Silencing S100PBP impairs RhoB signaling and promotes cell migration and invasion

a) Western blot analysis was conducted on Panc1 and MIA PaCa-2 cells after transient silencing of S100PBP using two distinct siRNAs (S100PBP mol1 and mol2). The expression of RhoA, RhoB, p-MYPT1-S696, MYPT1, p-cofilin-S3, cofilin, and GAPDH was measured. The fold change in protein expression relative to control cells is indicated above the blots based on densitometric analysis.

b) The distribution of F-actin and average signal intensity per cell in the indicated cell lines were also analyzed. Arrows indicate stress fiber formation. Statistical analysis was performed using N = 3, mean ± SD. Differences were observed in Panc1 cells after S100PBP silencing when compared to Panc1_Scram (*p < 0.05) and MIA PaCa-2 cells after silencing S100PBP versus MIA PaCa-2_Scram (†p < 0.05).

c) A time-lapse microscopy assay showed increased migration in Panc1 and MIA PaCa-2 cells upon S100PBP silencing with siRNA mol2. DAPI staining was used to track the nuclei.

d) Invasion was measured by a Matrigel invasion assay, where representative images of the inserts (top panel) and quantification of invading cells (bottom panel) were displayed.

EGFR-targeted CD73 internalization by bsAb CD73xEGFR

bsAb CD73xEGFR efficiently removes CD73 from cells expressing both CD73 and EGFR, whereas cells lacking EGFR show negligible CD73 internalization. Likewise, A549 EGFR-KO and H1650 EGFR-KO cells exhibited minimal CD73 uptake after treatment. Analysis across 10 CD73pos/EGFRpos cancer cell lines revealed a strong linear association (R^2=0.89) between residual surface CD73 and EGFR levels, whereas oleclumab treatment produced no correlation (R^2=0.0003) **(Figure 2h)**. These findings indicate that bsAb CD73xEGFR induces co-internalization of CD73 and EGFR on cancer cell surfaces.

After silencing S100PBP in Panc1 and MIA PaCa-2 cells (with siRNA mol2), both the 2D scratch wound assay and time-lapse microscopy revealed a substantial increase in the rate of migration **(Figure 2c),** suggesting that loss of S100PBP promotes cellular motility. Furthermore, the invasive potential of MIA PaCa-2 cells was also significantly enhanced in a Matrigel assay after S100PBP silencing **(Figure 2d)**. Similar increases in invasion were previously observed in Panc1 cells after S100PBP silencing [2], supporting the idea that S100PBP loss stimulates both migration and invasion.

To investigate the role of S100PBP in regulating cell movement further, we created stable cell lines (CFPac1 and PaTu-8988t) with S100PBP overexpression. These cell lines, which naturally express low levels of S100PBP **(Figure 3a)** displayed higher RhoB expression **(Figure 3a)**. These cells also exhibited a distinct round, tightly

packed, cobblestone-like morphology, in contrast to control cells, which retained an elongated, spindle-shaped form. Additionally, cells with high S100PBP levels showed a reduced rate of migration and invasion **(Figures 3c).** These findings confirm that S100PBP inhibits both cell motility and invasion.

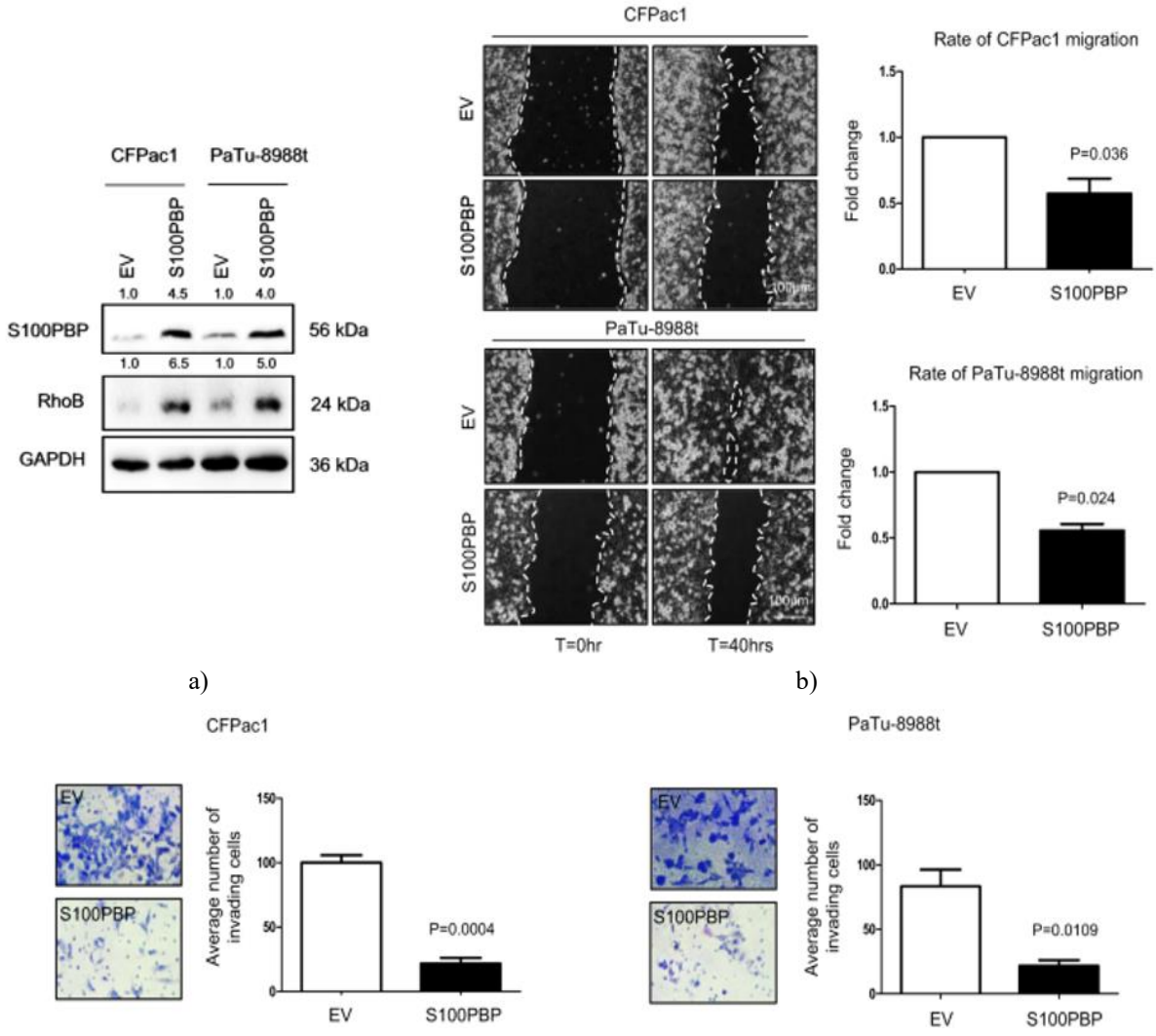

Figure 3: Persistent overexpression of S100PBP impedes cell migration and invasion

a) Expression levels of S100PBP and RhoB were evaluated in CFPac1 and PaTu-8988t cell lines after stable S100PBP overexpression. The EV control group, consisting of cells transduced with an empty vector, was used as a baseline. GAPDH served as the loading control. The numbers above the Western blot images indicate the fold changes in protein expression relative to the controls, as determined by densitometric analysis.

b, c) Both migration and invasion assays revealed a significant reduction in these processes in the S100PBP-overexpressing cells.

S100PBP interacts with p53 and affects apoptosis through AKT signaling

Pathway analysis (IPA) pointed to TP53 and AKT as key genes involved in cell movement after S100PBP deregulation **(Figure 1a).** Intriguingly, the levels of p53 in both PDAC and HAP1 cell lines followed the same pattern as S100PBP expression **(Figure 4a)**. Silencing S100PBP in Panc1 and MIA PaCa-2 cells led to decreased p53 at both the mRNA and protein levels **(Figure 4b)**, suggesting a regulatory link between

S100PBP and p53 expression. Since several S100 family proteins are known to interact with p53 [10, 11], we investigated whether S100PBP itself could bind p53. Co-immunoprecipitation experiments confirmed an interaction between the two proteins in Panc1 and MIA PaCa-2 cell lysates **(Figure 4c).** Moreover, p53 was predominantly located in the nucleus in both these cell lines, a pattern also observed in the S100PBP-overexpressing CFPac1 cells, indicating that the interaction occurs within the nucleus **(Figure 4d).**

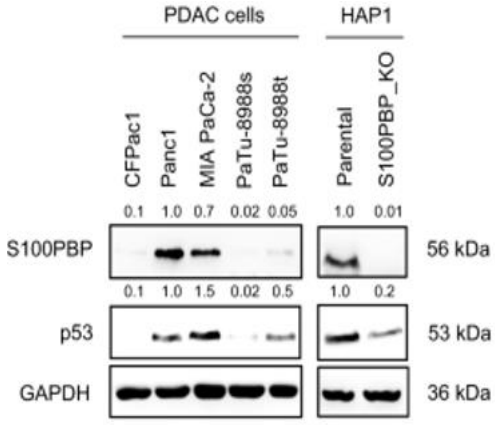

a)

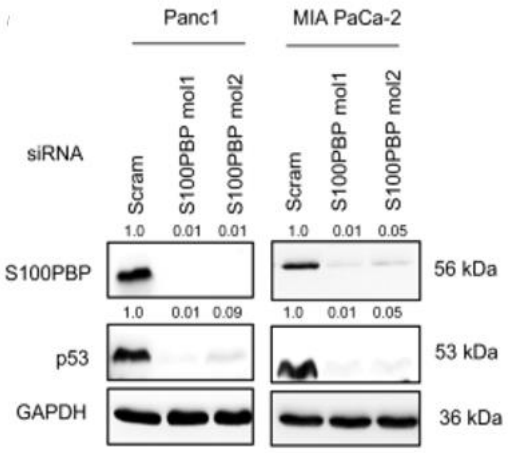

b)

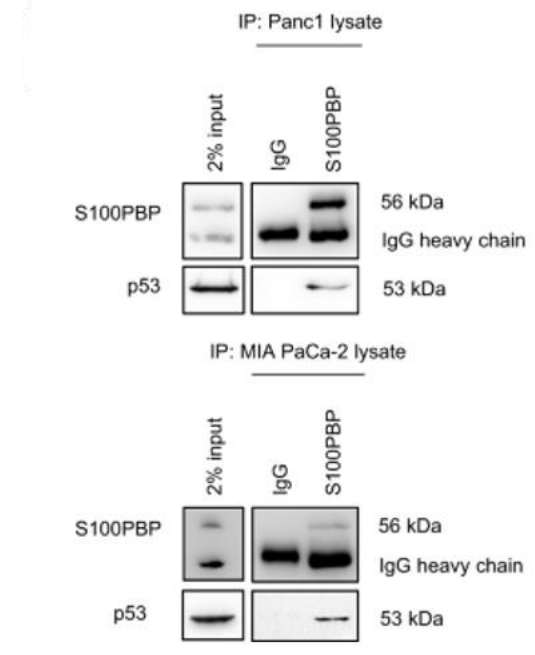

c)

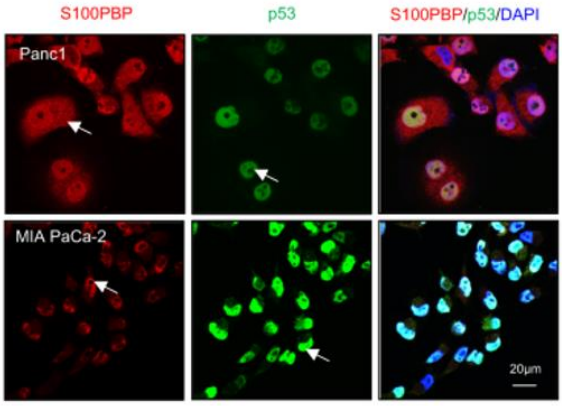

d)

Figure 4: Interaction of p53 and S100PBP Proteins. a) The levels of S100PBP and p53 were analyzed in a set of PDAC cell lines, including HAP1 cells with and without stable S100PBP knockout (KO). The cells were studied both before and after transient silencing using siRNA constructs (Scram, S100PBPmol1, and S100PBPmol2) in Panc1 and MIA PaCa-2 cells. GAPDH was used as a reference for equal loading. The numbers shown above the Western blot images represent fold changes in protein expression compared to the relevant controls (Panc1, HAP1-Parental, and Scram-transfected cells), as determined through densitometry.

b)After transient silencing, S100PBP and p53 expression levels were measured in Panc1 and MIA PaCa-2 cells.

c) A co-immunoprecipitation analysis was performed to evaluate the interaction between S100PBP and p53 proteins from Panc1 (top panel) and MIA PaCa-2 (bottom panel) lysates. Rabbit-IgG was included as a negative control, with 2% of the whole-cell lysate used as input.

d) The cellular localization of S100PBP and p53 was examined in Panc1 and MIA PaCa-2 cells. Nuclei were stained with DAPI. The arrows indicate the locations where both proteins co-localize in the nucleus, suggesting they interact within this compartment.

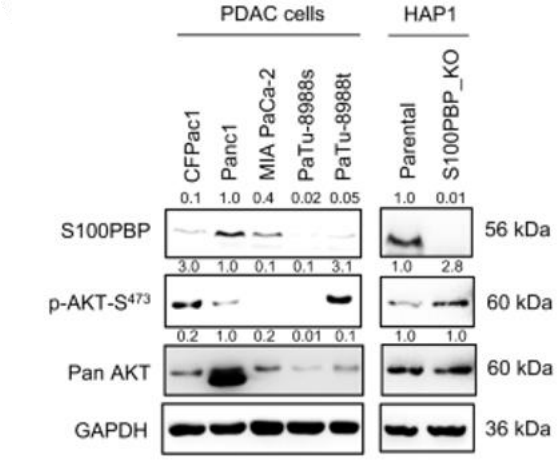

a)

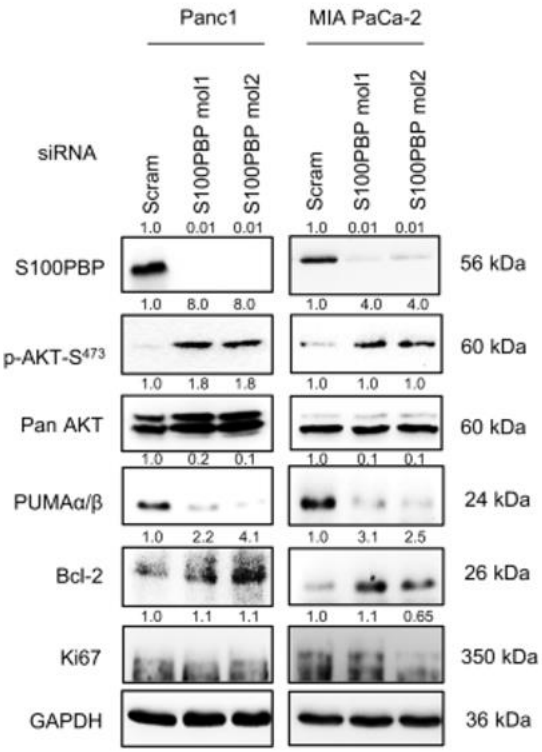

b)

We then investigated whether S100PBP could influence AKT signaling, as proposed in **Figure 1b**. A notable activation of the AKT pathway, as indicated by the increased phosphorylation of AKT at Ser473, was observed in cells expressing low levels of S100PBP **(Figure 5a**). This finding was consistent with the results from silencing S100PBP in Panc1 and MIA PaCa-2 cells, where p53 levels were reduced **(Figure 4b)**, alongside a downregulation of its target PUMAα/β, an increase in AKT activity, and an upregulation of Bcl-2, an anti-apoptotic protein **(Figure 5b)**. No significant change in Ki67 levels was observed, implying that the activation of AKT signaling was independent of its role in promoting cell proliferation **(Figure 5b).** To explore the impact of AKT activation on apoptosis, FITC-Annexin V flow cytometry was performed on Panc1 and MIA PaCa-2 cells with S100PBP knockdown, followed by gemcitabine treatment (0.01 µM for 96 hours). The results showed a significant reduction in apoptotic cells in the S100PBP-deficient population **(Figure 5c)**, supporting a role for S100PBP in modulating apoptosis via AKT signaling.

To further confirm these findings, we used PDAC cells overexpressing S100PBP. These cells exhibited elevated levels of p53 and decreased levels of p-AKT-S473 **(Figure 6a)**. Additionally, treatment of CFPac1 and PaTu-8988t control cells and their S100PBP-overexpressing counterparts with gemcitabine (0.01 µM for 96 hours) revealed a significant increase in apoptosis in the high-S100PBP-expressing cells **(Figure 6b)**. Further, increased cleavage of caspase-3 and PARP in these cells suggested that S100PBP may enhance chemosensitivity by promoting apoptosis.

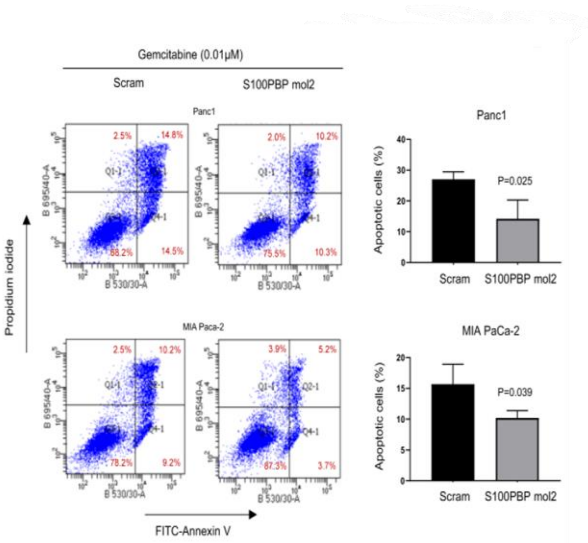

c)

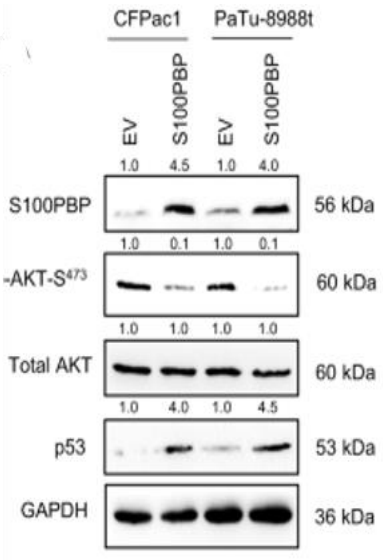

a)

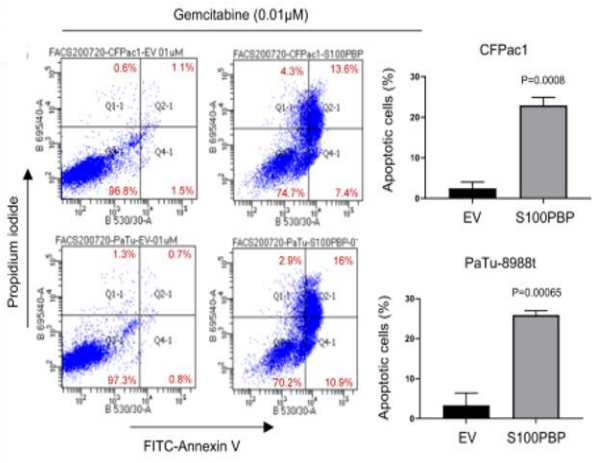

b)

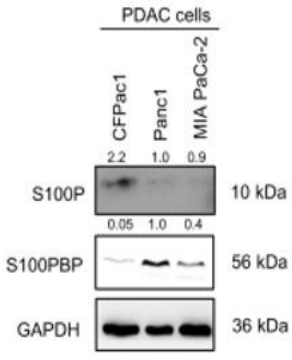

c)

Figure 5: Inverse Relationship Between AKT Activation and S100PBP Expression.

a) The levels of S100PBP, phosphorylated AKT (p-AKT-S473), and total AKT were measured in a range of PDAC and HAP1 cells (parental vs. S100PBP knockout (KO)), both before and after transient silencing of S100PBP using siRNA molecules (mol1 and mol2) in Panc1 and MIA PaCa-2 cell lines. Additionally, changes in the expression of PUMAα/β and Bcl-2 were evaluated. No significant differences in Ki67 expression were observed. GAPDH served as a loading control. Cells transfected with scrambled (non-target) siRNA were used as controls. The numbers displayed above the Western blot bands represent the fold changes in protein levels relative to the control groups (Panc1, HAP1-Parental, and Scram siRNA-transfected cells), determined via densitometric analysis.

b) After transient silencing, there was a reduction in PUMAα/β expression and an increase in Bcl-2, with no change in Ki67 levels.

c) Flow cytometry using FITC-Annexin V and Propidium iodide revealed a higher proportion of apoptotic cells in Panc1 and MIA PaCa-2 cells with silenced S100PBP (mol2), treated with gemcitabine (0.01 μM) for 96 hours.

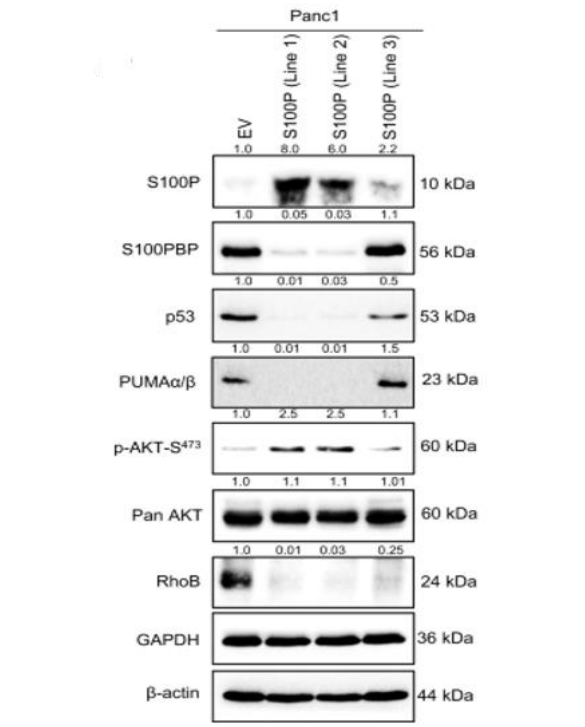

d)

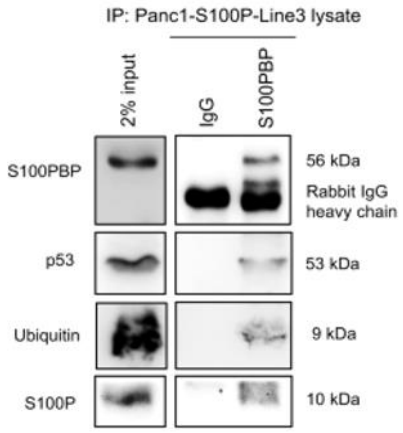

e)

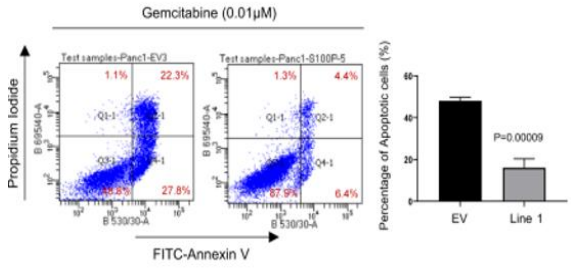

f)

Figure 6. S100PBP Reduces Cell Survival, While S100P Increases Cancer Cell Survival by Suppressing S100PBP.

a) The levels of S100PBP, p-AKT-S473, total AKT, and p53 were analyzed in CFPac1 and PaTu-8988 cells that stably overexpress S100PBP. Cells treated with an empty vector (EV) were used as controls. GAPDH served as the loading control.

b) After gemcitabine treatment (0.01 μM for 96 hours), there was a marked increase in apoptotic cells in the S100PBP-expressing cell population, as detected by FITC-Annexin V/Propidium iodide flow cytometry.

c) A reverse expression pattern of S100P and S100PBP was observed in PDAC cell lines (CFPac1, Panc1 (control), and MIA PaCa-2), with GAPDH as the loading control.

d) The levels of S100P, S100PBP, p53, PUMAα/β, p-AKT-S473, total AKT, and RhoB were examined in three Panc1 cell lines (Line 1, 2, and 3) that stably overexpress S100P. Control cells transduced with an empty vector (EV) were used as a reference. GAPDH and β-actin served as loading controls. The numbers above the Western blots represent the fold changes in protein expression compared to the controls, as quantified by densitometric analysis.

e) Immunoprecipitation (IP) of S100PBP, followed by the detection of p53, ubiquitin, and S100P proteins, was conducted using Panc1-S100P Line 3 lysates. Rabbit-IgG was used as a control, and 2% of the total lysate was used as input.

f) A reduction in apoptotic cells was observed in Panc1-S100P (Line 1) cells after treatment with gemcitabine (0.01 μM) for 96 hours, as detected by FITC-Annexin V/Propidium iodide flow cytometry.

S100 proteins, including S100P, play key roles in regulating p53 through post-translational modifications, stability, and cellular trafficking [12, 13]. As S100P expression increases while S100PBP levels decrease during PDAC progression [2], we sought to explore how S100P influences S100PBP expression. Western blot data, in line with previous histological findings, revealed that Panc1 and MIA PaCa-2 cells, which highly express S100PBP, had very low levels of S100P. This was in contrast to CFPac1 cells, which showed high levels of S100P **(Figure 6c)**. To further explore this, we established three Panc1 cell lines with stable S100P overexpression: Line 1 and Line 2, both of which express high levels of S100P, and Line 3, which expresses low levels **(Figure 6d)**. These cell lines and the EV control cells showed that Lines 1 and 2 had lower levels of S100PBP, p53, PUMAα/β, and RhoB, with elevated

AKT activation **(Figure 6d)**. Notably, cells with high S100P expression (Lines 1 and 2) showed a distinct morphological shift, transitioning from cuboidal, cobblestone-like shapes in control cells to elongated, spindle-shaped forms. There were no significant changes in S100PBP mRNA levels, indicating that the observed protein changes were not due to transcriptional regulation**.**

For further confirmation, Panc1 Line 3, which expresses low S100P but high S100PBP, was used in immunoprecipitation experiments. These confirmed the interaction between S100PBP and p53. Co-immunoprecipitation of S100P and ubiquitin in the same samples suggested that both S100PBP and p53 could be targeted for degradation **(Figure 6e)**. This suggests a dynamic, transient interaction between S100P, S100PBP, and p53, which could explain the inverse expression patterns observed in vitro and in tissue sections, as noted previously [1, 2].

The functional role of AKT activation in S100P-expressing cells was assessed by treating control and Line 1 cells with gemcitabine (0.01 µM for 96 hours) and performing FITC-Annexin V apoptotic assays. The results showed a significant reduction in apoptosis in the S100P-expressing cells (Line 1) compared to controls **(Figure 6f)**, indicating that S100P enhances chemoresistance.

KrasG12D Regulates S100PBP Expression through Epigenetic Pathways

Mutant KRAS is a well-known regulator of various S100 proteins in cancer [14, 15], and it plays a critical role in the early stages of PDAC development. To investigate whether KrasG12D affects S100PBP expression, we used doxycycline-inducible KrasG12D PDAC mouse cell lines (iKrasG12Dp53L/+) [7]. Activation of KrasG12D led to a reduction in S100PBP expression **(Figure 7a)** and caused S100PBP to translocate to the cytoplasm **(Figure 7b)**, which mirrors the patterns observed in human PanIN lesions [1, 2]. These results suggest that KrasG12D regulates S100PBP through epigenetic mechanisms.

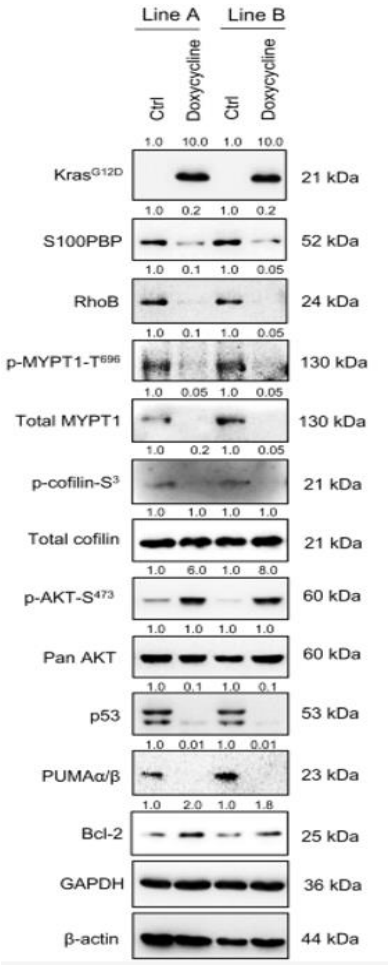

a)

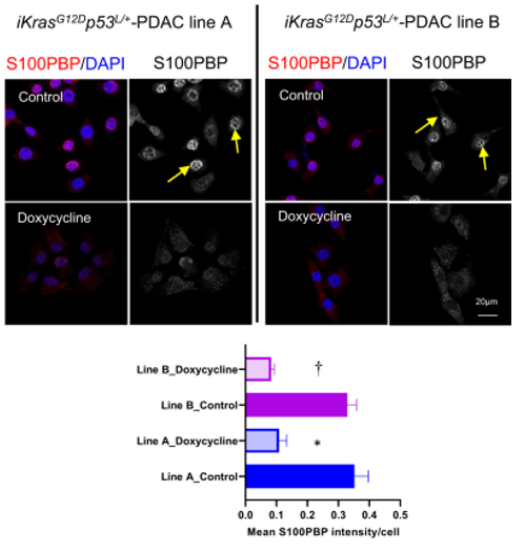

b)

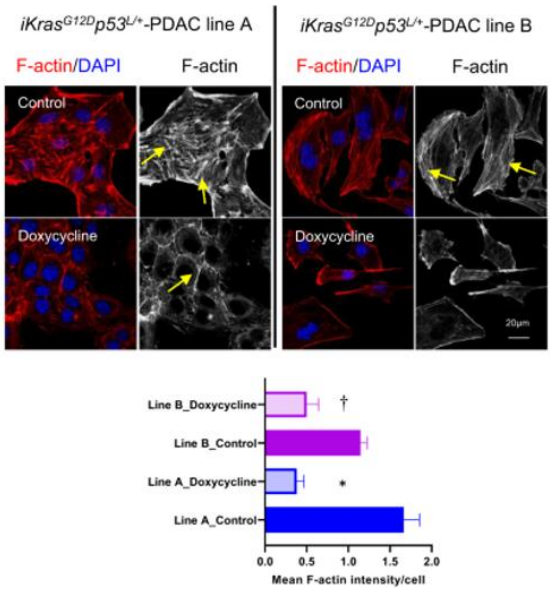

c)

Figure 7: KrasG12D Activation Reduces S100PBP Expression and Promotes AKT Activation.

A The expression of various proteins—KrasG12D, S100PBP, RhoB, p-MYPT1-S696, total MYPT1, p-cofilin-S3, total cofilin, p-AKT-S473, total AKT, p53, PUMAα/β, and Bcl-2—was examined in two iKras mouse PDAC cell lines (A and B) after a 24-hour doxycycline (1 μg/mL) treatment. GAPDH and β-actin were used as internal controls.

B The translocation of S100PBP (denoted by arrows) from the nuclei (indicated by DAPI staining) to the cytoplasm was observed in doxycycline-treated iKras cells, in contrast to untreated control cells.

C Changes in F-actin organization and the mean signal intensity per cell were analyzed in the same cell lines. Arrows highlight areas with strong cortical staining and stress fiber formation. Data are presented as the mean ± SD from three independent experiments, with statistical comparisons between doxycycline-treated and control groups: *$p < 0.05$ for Line A_Doxycycline vs. Line A_Control, and †$p < 0.05$ for Line B_Doxycycline vs. Line B_Control. Western blot numbers indicate fold changes in protein expression relative to controls, based on densitometric analysis.

KrasG12D activation led to a decrease in RhoB, p-MYPT1-S696, and p-cofilin-S3, which indicates suppression of the RhoB signaling pathway **(Figure 7a)**. Additionally, in response to KrasG12D activation, F-actin cortical staining appeared weak and disorganized, with marked formation of stress fibers across the cell surface **(Figure 7c)**. This reorganization was accompanied by a shift in cellular shape, with control cells showing a round, cobblestone-like morphology, while KrasG12D-activated cells took on a more elongated, spindle-shaped appearance. Furthermore, KrasG12D activation led to the depletion of p53 and PUMAα/β, while increasing Bcl-2 levels and activating pro-survival AKT signaling **(Figure 7a)**. These findings highlight S100PBP as a target of KrasG12D activation, suggesting that its loss is a critical step in the development and progression of PDAC.

Given previous reports of elevated class-I histone deacetylase (HDAC) activity driven by mutant KRAS in PDAC [16, 17], and the identification of HDAC in the IPA signaling network **(Figure 1b)**, we investigated the potential role of HDACs in regulating S100PBP expression. When CFPac1 and PaTu-8988t cells were treated with the class-I HDAC inhibitor MS-275/Entinostat [18], S100PBP expression and acetylated histone H3 levels were restored in a dose-dependent manner **(Figure 8a).** Additionally, pre-treatment of KrasG12D PDAC mouse cell line-A with 0.2 μM MS-275 also led to an increase in S100PBP and acetyl lysine levels **(Figure 8b)**. While doxycycline-induced KrasG12D activation led to reduced S100PBP expression, pre-treatment with 0.2 μM MS-275 largely reversed these effects, maintaining S100PBP levels similar to untreated controls **(Figure 8b)**. These results indicate that KrasG12D-mediated regulation of S100PBP involves, at least in part, epigenetic mechanisms.

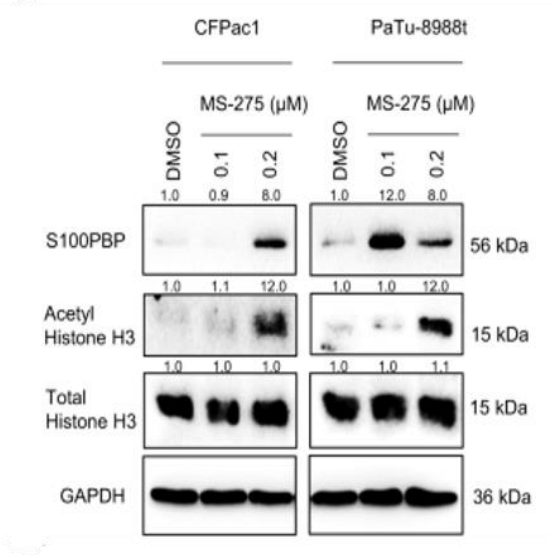

a)

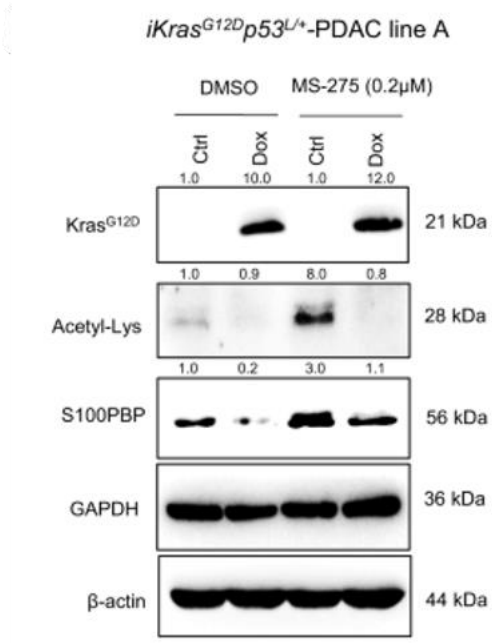

b)

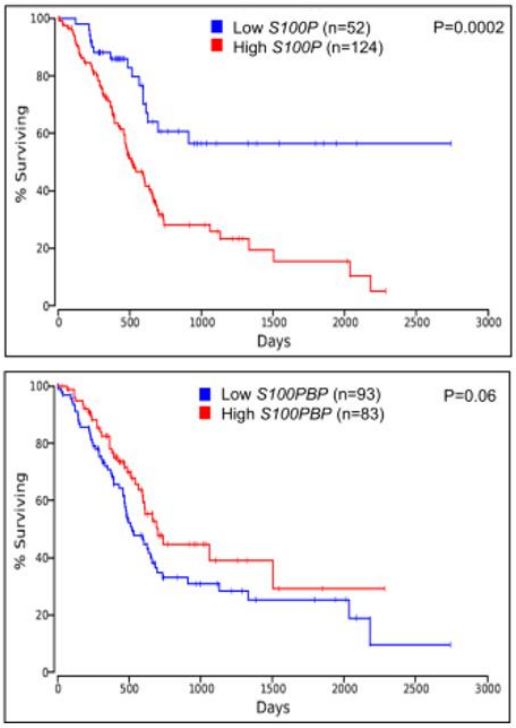

c)

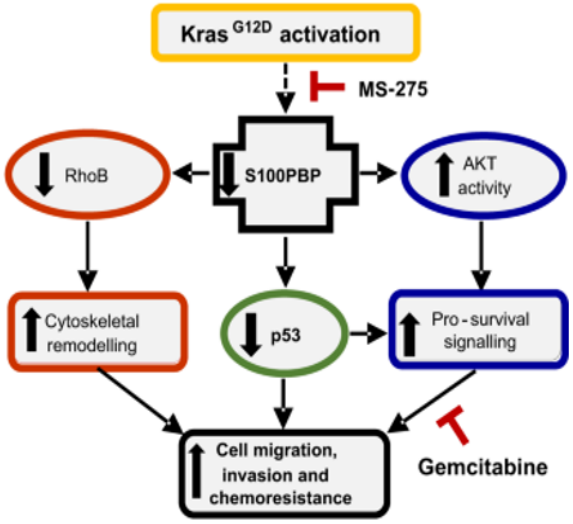

d)

Figure 8. Restoring S100PBP Expression by Inhibiting HDAC Activity.

a) The levels of S100PBP, acetylated histone H3, and total histone H3 were measured in cell lysates from CFPac1 and PaTu-8988t cells after treatment with 0.1 or 0.2 μM MS-275 or the vehicle control (DMSO) for 72 hours. The results show that MS-275 treatment restores S100PBP expression in both cell lines.

b)Western blot analysis of KrasG12D, S100PBP, and acetyl-lysine levels in lysates from iKras mouse PDAC cells after 24 hours of pre-treatment with 0.2 μM MS-275, followed by 24 hours of doxycycline (1 μg/mL) treatment. This experiment demonstrates the epigenetic modification of S100PBP by KrasG12D activation. GAPDH and β-actin were used as internal controls. Numbers above the Western blots indicate fold changes in protein expression relative to controls, based on densitometric analysis.

c) Kaplan-Meier survival curves were generated using data from the TCGA PanCancer Atlas, which includes 176 patients with pancreatic adenocarcinoma. The survival analysis reveals that patients exhibiting high S100P and low S100PBP expression have significantly poorer survival outcomes.

d) A schematic diagram depicting the KrasG12D/S100PBP signaling pathway in PDAC cells.

High S100P Expression and Low S100PBP Expression Correlate with Poor Prognosis

To assess the clinical significance of S100P and S100PBP, we analyzed the TCGA PanCancer Atlas dataset from 176 pancreatic adenocarcinoma patients,

generating Kaplan-Meier survival plots **(Figure 8c)**. These results show a clear association between high S100P expression and low S100PBP levels with decreased survival rates.

In this study, we highlight novel tumor-suppressive functions of S100PBP, including its role in modulating cell morphology, motility, invasion, and cytoskeletal organization. We show that these effects are mediated by the RhoB GTPase and its downstream targets, ROCK-1/2, which are involved in regulating the stability of F-actin filaments, thereby influencing processes like cell shape and movement [19, 20]. We have previously observed that the overexpression of S100P in PDAC cells disrupts actin polymerization and F-actin cortical localization, thereby promoting motility and invasion [6]. In the present study, we extend these findings to S100PBP, showing that reduced S100PBP expression—whether by endogenous expression or gene silencing—results in weaker F-actin cortical staining and the loss of stress fibers. These alterations are linked to enhanced cell motility and invasion, as seen in previous studies of cells with low F-actin polymerization and cortical localization [21- 23]. Furthermore, we observed a direct relationship between RhoB and S100PBP expression in PDAC and CML cells. RhoB downregulation, which promotes migration and invasiveness, further supports the role of S100PBP in regulating the cytoskeleton and cell movement through RhoB signaling.

While RhoA and RhoC are commonly associated with oncogenic activity [17, 24], RhoB has been identified as a tumor suppressor in pancreatic and other cancers [25-28]. RhoB-deficient mice show a higher incidence of Ras-driven tumors, and its loss enhances the metastatic spread of lung cancer cells, a process mediated by AKT signaling [25]. Additionally, the downregulation of RhoB by oncogenic Ras through PI3K/AKT signaling [29] supports the notion that S100PBP functions within this same signaling network. The low expression of RhoB in human PDAC samples further reinforces the hypothesis that S100PBP plays a tumor-suppressive role through the regulation of RhoB signaling.

The involvement of p53 in controlling cell migration and morphology by suppressing cell polarization, protrusion formation, and spreading has been well documented [30-33]. Several studies have shown that p53 suppresses cell migration and metastasis, and these functions are largely mediated through its regulation of the actin cytoskeleton via Rho signaling pathways [34, 35]. In pancreatic cancer, the loss of p53 function leads to cell cycle dysregulation, evasion of apoptosis, and accelerated disease progression [12, 36- 39]. Our findings further substantiate the role of S100PBP in modulating cytoskeletal dynamics and cell motility through the p53/RhoB pathway, suggesting that S100PBP contributes to the suppression of PDAC progression and metastasis.

Our results indicate that S100PBP plays a dual role in regulating TP53—both at the transcriptional level and through direct interaction with p53 in the nucleus. Previous research has established that S100P, along with other members of the S100 protein family, binds to p53, influencing its oligomerization, stability, and trafficking, which in turn regulates its activity [10-12]. For the first time, we show that S100PBP also binds p53, and forms a complex involving S100PBP, p53, S100P, and ubiquitin. This complex may be critical for the destabilization and/or degradation of both S100PBP and p53. While further experiments are required to define the precise mechanisms involved in their ubiquitination and proteasomal degradation, we speculate that this process may be active in vivo during PDAC progression, as suggested by the loss of S100PBP observed in PanIN stages. The loss of S100PBP would 'release' S100P—an invasive protein—that can disrupt p53 activity, promoting the metastatic spread of PDAC cells. The oncogenic role of S100P in neutralizing p53 and driving aggressive tumor growth has been highlighted in previous studies [11].

It is well-known that the loss of p53 expression is linked to increased PI3K and AKT activity, a hallmark of many cancers [40, 41]. AKT hyperactivation promotes tumor growth, evasion of apoptosis, and resistance to chemotherapy [42, 43]. In PDAC, AKT expression is elevated by approximately 50%, and its overexpression is a poor prognostic indicator [44, 45]. We observed that AKT activation (indicated by pAKT-S473 levels) inversely correlates with S100P and S100PBP expression in all PDAC cell lines studied. Overexpression of S100PBP in PDAC cells reduced AKT activation and enhanced sensitivity to Gemcitabine, whereas silencing S100PBP in cells with low S100P (e.g., MIA PaCa-2 and Panc1) increased AKT activity, suggesting that low S100PBP expression confers intrinsic chemoresistance. These findings are consistent with earlier research on Panc1 cells, where inhibiting phosphorylated FAK led to decreased AKT activation and increased Gemcitabine-induced cell death [46].

Given that KRAS mutations are the initiating events in PDAC, we hypothesized that KrasG12D could directly or indirectly impact S100PBP signaling. Indeed, activation of KrasG12D in inducible KRAS-driven mouse models of PDAC led to reduced S100PBP levels and its relocation from the nucleus to the cytoplasm. Moreover, the downstream effects of KrasG12D on RhoB, AKT, and p53 signaling closely mirrored the effects observed after silencing S100PBP, thus confirming that KRAS is an upstream regulator of the S100PBP signaling axis, as shown in **Figure 8d**.

In various cancers, including PDAC, overactive KRAS has been shown to suppress pro-apoptotic and tumor suppressor genes through epigenetic modifications of histones [47-50]. The upregulation of class-I HDACs in PDAC has been reported previously [16, 51]. We show that treatment with the class-I HDAC inhibitor MS-275 can partially restore S100PBP expression in vitro, by reversing the KrasG12D-induced suppression of S100PBP. This suggests that S100PBP expression is regulated through epigenetic mechanisms, as previously observed for S100P [52]. HDAC inhibitors such as vorinostat have demonstrated promising results in enhancing tumor cell death and reducing the progression of pancreatic cancer [47, 49, 50, 53], and our study now links S100PBP to the mechanisms underlying these effects. Further studies investigating the role of specific class-I HDACs in regulating S100PBP expression could provide valuable insights into potential therapeutic strategies.

Conclusion

In conclusion, we present a novel role for S100PBP as a tumor suppressor in PDAC, regulating cellular morphology, motility, invasion, and survival. S100PBP functions as a critical signaling molecule in the Kras/AKT/RhoB/p53 pathway and is likely regulated epigenetically. Given that high S100P expression and low S100PBP expression correlate with poor prognosis in PDAC patients, these findings underscore the potential clinical relevance of S100PBP as a therapeutic target in pancreatic cancer.

Acknowledgments: The inducible iKras PDAC mouse model was generated by Prof. Ronald DePinho's Laboratory (MD Anderson Cancer Center, Houston, TX), and the iKras PDAC cell-lines isolated from this model were a gift from Dr. Faraz Mardakheh (Barts Cancer Institute). The authors would also like to thank Flow cytometry Core facility team at Barts Cancer Institute for the training and support provided towards this study.

Conflict of Interest: None

Financial Support: None

Ethics Statement: None

References

1. Dowen SE, Crnogorac-Jurcevic T, Gangeswaran R, Hansen M, Eloranta JJ, Bhakta V, et al. Expression of S100P and its novel binding partner S100PBPR in early pancreatic cancer. Am J Pathol. 2005;166:81–92.
2. Lines KE, Chelala C, Dmitrovic B, Wijesuriya N, Kocher HM, Marshall JF, et al. S100P-binding protein, S100PBP, mediates adhesion through regulation of cathepsin Z in pancreatic cancer Cells. Am J Pathol. 2012;180:1485–94.
3. Lu YJ, Yang Y, Hu TH, Duan WM. Identification of key genes and pathways at the downstream of S100PBP in pancreatic cancer cells by integrated bioinformatical analysis. Transl Cancer Res. 2021;10:806–16.
4. Xie H, Lee L, Scicluna P, Kavak E, Larsson C, Sandberg R, et al. Novel functions and targets of miR-944 in human cervical cancer cells. Int J Cancer. 2015;136:E230–41.
5. Yang PS, Hsu HH, Hsu TC, Chen MJ, Wang CD, Yu SL, et al. Genome-wide scan for copy number alteration association with relapse-free survival in colorectal cancer with liver metastasis patients. J Clin Med. 2018;7:446.
6. Whiteman HJ, Weeks ME, Dowen SE, Barry S, Timms JF, Lemoine NR, et al. The role of S100P in the invasion of pancreatic cancer cells is mediated through cytoskeletal changes and regulation of cathepsin D. Cancer Res. 2007;67:8633–42.
7. Ying HQ, Kimmelman AC, Lyssiotis CA, Hua SJ, Chu GC, Fletcher-Sananikone E, et al. Oncogenic Kras maintains pancreatic tumors through regulation of anabolic glucose metabolism. Cell. 2012;149:656–70.
8. Srivastava K, Pickard A, Craig SG, Quinn GP, Lambe SM, James JA, et al. Delta Np63

gamma/SRC/Slug signaling axis promotes epithelial-to-mesenchymal transition in squamous cancers. Clin Cancer Res. 2018;24:3917–27.
9. Srivastava K, Shao B, Bayraktutan U. PKC-beta exacerbates in vitro brain barrier damage in hyperglycemic settings via regulation of RhoA/Rho-kinase/MLC2 pathway. J Cereb Blood Flow Metab. 2013;33:1928–36.
10. Srivastava K, Pickard A, McDade S, McCance DJ. p63 drives invasion in keratinocytes expressing HPV16 E6/E7 genes through regulation of Src-FAK signalling. Oncotarget. 2017;8:16202–19
11. van Dieck J, Fernandez-Fernandez MR, Veprintsev DB, Fersht AR. Modulation of the oligomerization state of p53 by differential binding of proteins of the S100 family to p53 monomers and tetramers. J Biol Chem. 2009;284:13804–11.
12. Fernandez-Fernandez MR, Veprintsev DB, Fersht AR. Proteins of the S100 family regulate the oligomerization of p53 tumor suppressor. Proc Natl Acad Sci USA. 2005;102:4735–40.
13. Gibadulinova A, Pastorek M, Filipcik P, Radvak P, Csaderova L, Vojtesek B, et al. Cancer-associated S100P protein binds and inactivates p53, permits therapy-induced senescence and supports chemoresistance. Oncotarget. 2016;7:22508–22.
14. Woo T, Okudela K, Mitsui H, Tajiri M, Rino Y, Ohashi K, et al. Up-regulation of S100A11 in lung adenocarcinoma-its potential relationship with cancer progression. PLoS ONE. 2015;10:e0142642.
15. Bydoun M, Sterea A, Liptay H, Uzans A, Huang WY, Rodrigues GJ, et al. S100A10, a novel biomarker in pancreatic ductal adenocarcinoma. Mol Oncol. 2018;12:1895–916.
16. Cai MH, Xu XG, Yan SL, Sun Z, Ying Y, Wang BK, et al. Depletion of HDAC1, 7 and 8 by histone deacetylase inhibition confers elimination of pancreatic cancer stem cells in combination with gemcitabine. Sci Rep. 2018;8:1621.
17. von Burstin J, Eser S, Paul MC, Seidler B, Brandl M, Messer M, et al. E-cadherin regulates metastasis of pancreatic cancer in vivo and is suppressed by a SNAIL/HDAC1/HDAC2 repressor complex. Gastroenterology. 2009;137:361–71.
18. Peulen O, Gonzalez A, Peixoto P, Turtoi A, Mottet D, Delvenne P, et al. The Anti-tumor effect of HDAC inhibition in a human pancreas cancer model is significantly improved by the simultaneous inhibition of cyclooxygenase 2. PLoS ONE. 2013;8:e75102.
19. Ellenbroek SIJ, Collard JG. Rho GTPases: functions and association with cancer. Clin Exp Metastasis. 2007;24:657–72.
20. Karlsson R, Pedersen ED, Wang Z, Brakebusch C. Rho GTPase function in tumorigenesis. Biochim Biophys Acta. 2009;1796:91–8.
21. Bousquet E, Calvayrac O, Mazieres J, Lajoie-Mazenc I, Boubekeur N, Favre G, et al. RhoB loss induces Rac1-dependent mesenchymal cell invasion in lung cells through PP2A inhibition. Oncogene. 2016;35:1760–9.
22. Wicki A, Lehembre F, Wick N, Hantusch B, Kerjaschki D, Christofori G. Tumor invasion in the absence of epithelial-mesenchymal transition: podoplanin-mediated remodeling of the actin cytoskeleton. Cancer Cell. 2006;9:261–72.
23. Morris HT, Machesky LM. Actin cytoskeletal control during epithelial to mesenchymal transition: focus on the pancreas and intestinal tract. Br J Cancer. 2015;112:613–20.
24. Suwa H, Ohshio G, Imamura T, Watanabe G, Arii S, Imamura M, et al. Overexpression of the RhoC gene correlates with progression of ductal adenocarcinoma of the pancreas. Br J Cancer. 1998;77:147–52
25. Bousquet E, Mazieres J, Privat M, Rizzati V, Casanova A, Ledoux A, et al. Loss of RhoB expression promotes migration and invasion of human bronchial cells via activation of AKT1. Cancer Res. 2009;69:6092–9.
26. Tan YG, Yin HZ, Zhang HY, Fang J, Zheng W, Li D, et al. Sp1-driven up-regulation of miR-19a decreases RhoB and promotes pancreatic cancer. Oncotarget. 2015;6:17391–403.
27. Marlow LA, Reynolds LA, Cleland AS, Cooper SJ, Gumz ML, Kurakata S, et al. Reactivation of suppressed RhoB is a critical step for the inhibition of anaplastic thyroid cancer growth. Cancer Res. 2009;69:1536–44.
28. Huang M, Prendergast GC. RhoB in cancer suppression. Histol Histopathol. 2006;21:213–8.
29. Jiang K, Sun JZ, Cheng J, Djeu JY, Wei S, Sebti S. Akt mediates Ras downregulation of RhoB, a suppressor of transformation, invasion, and metastasis. Mol Cell Biol. 2004;24:5565–76.

30. Roger L, Gadea G, Roux P. Control of cell migration: a tumour suppressor function for p53? Biol Cell. 2006;98:141–52.
31. Gadea G, Roger L, Anguille C, de Toledo M, Gire V, Roux PTNF. alpha induces sequential activation of Cdc42-and p38/p53-dependent pathways that antagonistically regulate filopodia formation. J Cell Sci. 2004;117:6355–64.
32. Gadea G, Lapasset L, Gauthier-Rouviere C, Roux P. Regulation of Cdc42-mediated morpholigical effects: a novel function for p53. EMBO J. 2002;21:2373–82.
33. Alexandrova A, Ivanov A, Chumakov P, Kopnin B, Vasiliev J. Changes in p53 expression in mouse fibroblasts can modify motility and extracellular matrix organization. Oncogene. 2000;19:5826–30.
34. Hwang CI, Matoso A, Corney DC, Flesken-Nikitin A, Korner S, Wang W, et al. Wild-type p53 controls cell motility and invasion by dual regulation of MET expression. Proc Natl Acad Sci USA. 2011;108:14240–5.
35. Chen YW, Klimstra DS, Mongeau NE, Tatem JL, Boyartchuk V, Lewis BC. Loss of p53 and Ink4a/Arf cooperate in a cell autonomous fashion to induce metastasis of hepatocellular carcinoma cells. Cancer Res. 2007;67:7589–96.
36. Mello SS, Valente LJ, Raj N, Seoane JA, Flowers BM, McClendon J, et al. A p53 super-tumor suppressor reveals a tumor suppressive p53-Ptpn14-Yap axis in pancreatic cancer. Cancer Cell. 2017;32:460–73.
37. Hezel AF, Kimmelman AC, Stanger BZ, Bardeesy N, DePinho RA. Genetics and biology of pancreatic ductal adenocarcinoma. Genes Dev. 2006;20:1218–49.
38. Maitra A, Adsay NV, Argani P, Iacobuzio-Donahue C, De Marzo A, Cameron JL, et al. Multicomponent analysis of the pancreatic adenocarcinoma progression model using a pancreatic intraepithelial neoplasia tissue microarray. Mod Pathol. 2003;16:902–12.
39. Boschman CR, Stryker S, Reddy JK, Rao MS. Expression of p53 protein in precursor lesions and adenocarcinoma of human pancreas. Am J Pathol. 1994;145:1291–5.
40. Guo FK, Gao Y, Wang L, Zheng Y. P19(Arf)-p53 tumor suppressor pathway regulates cell motility by suppression of phosphoinositide 3-kinase and Rac1 GTPase activities. J Biol Chem. 2003;278:14414–9.
41. Higuchi M, Masuyama N, Fukui Y, Suzuki A, Gotoh Y. Akt mediates Rac/Cdc42-regulated cell motility in growth factor-stimulated cells and in invasive PTEN knockout cells. Curr Biol. 2001;11:1958–62.
42. Wheeler DL, Dunn EF, Harari PM. Understanding resistance to EGFR inhibitors-impact on future treatment strategies. Nat Rev Clin Oncol. 2010;7:493–507.
43. Vara JAF, Casado E, de Castro J, Cejas P, Belda-Iniesta C, Gonzalez-Baron M. PI3K/Akt signalling pathway and cancer. Cancer Treat Rev. 2004;30:193–204.
44. Edling CE, Selvaggi F, Buus R, Maffucci T, Di Sebastiano P, Friess H, et al. Key role of phosphoinositide 3-Kinase class IB in pancreatic cancer. Clin Cancer Res. 2010;16:4928–37.
45. Yamamoto S, Tomita Y, Hoshida Y, Morooka T, Nagano H, Dono K, et al. Prognostic significance of activated Akt expression in pancreatic ductal adenocarcinoma. Clin Cancer Res. 2004;10:2846–50.
46. Wu HW, Liang ZY, Shi XH, Ren XY, Wang K, Liu TH. Intrinsic chemoresistance to gemcitabine is associated with constitutive and laminin-induced phosphorylation of FAK in pancreatic cancer cell lines. Mol Cancer. 2009;8:125.
47. Mazur PK, Herner A, Mello SS, Wirth M, Hausmann S, Sanchez-Rivera FJ, et al. Combined inhibition of BET family proteins and histone deacetylases as a potential epigenetics-based therapy for pancreatic ductal adenocarcinoma. Nat Med. 2015;21:1163–71.
48. Mou HW, Moore J, Malonia SK, Li YX, Ozata DM, Hough S, et al. Genetic disruption of oncogenic Kras sensitizes lung cancer cells to Fas receptor-mediated apoptosis. Proc Natl Acad Sci USA. 2017;114:3648–53.
49. Yamada T, Amann JM, Tanimoto A, Taniguchi H, Shukuya T, Timmers C, et al. Histone deacetylase inhibition enhances the antitumor activity of a MEK Inhibitor in lung cancer cells harboring RAS mutations. Mol Cancer Ther. 2018;17:17–25.
50. Morelli MP, Tentler JJ, Kulikowski GN, Tan AC, Bradshaw-Pierce EL, Pitts TM, et al. Preclinical activity of the rational combination of Selumetinib (AZD6244) in combination with Vorinostat in

KRAS-mutant colorectal cancer models. Clin Cancer Res. 2012;18:1051–62.

51. Mishra VK, Wegwitz F, Kosinsky RL, Sen M, Baumgartner R, Wulff T, et al. Histone deacetylase class-I inhibition promotes epithelial gene expression in pancreatic cancer cells in a BRD4-and MYC-dependent manner. Nucleic Acids Res. 2017;45:6334–49.
52. Wang Q, Williamson M, Bott S, Brookman-Amissah N, Freeman A, Nariculam J, et al. Hypomethylation of WNT5A, CRIP1 and S100P in prostate cancer. Oncogene. 2007;26:6560–5.
53. Ruscetti M, Dadashian EL, Guo W, Quach B, Mulholland DJ, Park JW, et al. HDAC inhibition impedes epithelial-mesenchymal plasticity and suppresses metastatic, castration-resistant prostate cancer. Oncogene. 2016;35:3781–95.